Polymer Vol. 39 No. 24 pp. 5879–5887, 1998
0032-3861/98/$ – see front matter

PII: S0032-3861(97)10200-2

polymer papers

Co-continuous morphologies in polymer blends: a new model

R. C. Willemse, A. Posthuma de Boer*, J. van Dam and A. D. Gotsis
Department of Polymer Technology, Delft University of Technology, Julianalaan 136, 2628 BL, Delft, The Netherlands
(Received 14 May 1997; revised 24 September 1997; accepted 30 October 1997)

A model for phase continuity in polymer blends based on geometrical requirements for co-continuous structures has been developed. The minor phase of a fully co-continuous blend is considered as a dispersion of randomly oriented rods at their maximum packing density in the major phase. An existing empirical relation between this packing density and the aspect ratio of the rods, in conjunction with micro-rheological requirements for the existence of such rods, results in an equation describing the critical volume fraction of the minor phase for complete co-continuity as a function of the matrix viscosity, interfacial tension, shear rate and phase dimensions. This equation naturally leads to a range of compositions within which fully co-continuous structures can exist. It is demonstrated that existing relations between the volume fraction at phase inversion and the viscosity ratio of the blend components are not generally valid. Experimental evidence obtained by blending of PS and PE shows that the new model quantitatively predicts trends in the critical volume fraction as a function of the viscosities of both phases. An absolute prediction is not yet possible because the phase dimensions cannot *a priori* be predicted, but have to be measured.

(Keywords: polymer blends; co-continuous morphology; phase inversion)

INTRODUCTION

Blending of polymers is an effective way to obtain materials with specific properties. Most polymers are immiscible, therefore, blending usually leads to heterogeneous morphologies. The type and dimensions of the morphology determine the properties of the blend. Droplet/matrix morphologies improve the impact properties[1–3], fibrillar morphologies result in better tensile properties[4–9], blends with a lamellar structure enhance barrier properties[10], and co-continuous morphologies show a combination of the characteristics of both polymer components[11–13].

The type of morphology which is formed during processing depends on the nature of the polymers (interfacial tension, viscosities and the ratio of these viscosities), their volume fractions and the processing conditions. Abundant literature exists concerning the formation of dispersed morphologies (e.g.[1–9]), but relatively little is known about the composition range and processing conditions at which co-continuity can be found[14–25]. Continuity of one phase within the other can occur at low volume fractions, depending on the shape of the dispersed particles[18]. In the case of spherical droplets, continuity (percolation) of the minor phase is possible above 16 vol% droplets, whereas this percolation threshold value is much lower in the case of fibres. The percolation threshold value, however, is only the volume fraction limit for the onset of continuity of the minor phase. Not all the material of the minor phase belongs to the percolating structure then. At increasing volume fraction, the proportion of the minor component incorporated in the percolating structure will increase until at a certain volume fraction all material of this component becomes part of the single percolating structure. In other words, by then a fully continuous phase of the minor component in the major phase is obtained, a fully co-continuous morphology. In this paper, only these fully co-continuous morphologies are considered.

Several relations have been reported giving the volume fraction at which co-continuity can be formed as a function of the viscosity ratio only[19–25]. These relations, however, give a volume fraction for phase inversion rather than a range of compositions at which co-continuity is possible. They do not take into account any requirements as to the shape of the dispersed component necessary to obtain co-continuity. Especially at low volume fractions, co-continuity can only exist if the minor blend component consists of structures with an extended shape. Only then is this component capable of forming a continuous network. This can be accomplished under appropriate blending conditions. For this reason, it is to be expected that the formation of a co-continuous morphology will be strongly dependent on the processing conditions and processing properties of the blend components. In this paper, a semi-empirical relation is derived giving the volume fraction limits for co-continuity as a function of matrix viscosity, interfacial tension and shear rate during blending. It is based on a simple picture of a co-continuous structure as a dense packing of randomly oriented rodlike particles of the minor phase, and on the micro-rheological requirements for the stability of such rods. The model is shown to be in quantitative agreement with experimental results for blends of polystyrene in polyethylene of various viscosities, blended at various conditions.

THEORY

Existing relations for co-continuity

Co-continuity occurs around the phase inversion point, where a dispersion of component 1 in a matrix of component

* To whom correspondence should be addressed

2 will change into a dispersion of component 2 in a matrix of component 1. In the literature, several empirical relations have been proposed to describe the point of phase inversion. The relation used most frequently was given by Paul and Barlow[19], Jordhamo et al.[20], and was later generalized by Miles and Zurek[21]:

$$\frac{\phi_1}{\phi_2} = \frac{\eta_1(\dot{\gamma})}{\eta_2(\dot{\gamma})} \tag{1}$$

where η_i $(\dot{\gamma})$ is the viscosity of component i at blending conditions and ϕ_i is its volume fraction at which phase inversion occurs. Avgeropoulos et al.[22] used the torque ratio instead of a viscosity ratio, thus including all stresses that act on the polymers during blending in a batch mixer, e.g. shearing and elongational stresses. Ho et al.[23] also found a relation between volume fraction and torque ratio. Assuming the torque ratio and viscosity ratio to be equal[22], Ho et al.'s[23] result can be written as:

$$\frac{\phi_1}{\phi_2} = 1.22\left(\frac{\eta_1(\dot{\gamma})}{\eta_2(\dot{\gamma})}\right)^{0.29} \tag{2}$$

This relation was found by a least square analysis of experimental data[23], explaining perhaps why inverting the designations, 1 and 2, does not give an identical result, as might be expected. The relations (1) and (2) are shown in *Figure 1*.

Several attempts were made to develop a theory which describes phase inversion in polymer blends. Metelkin and Blekht[25] used the theory of Tomotika[26] for the instability of a liquid cylinder surrounded by another liquid. At the point of phase inversion, the breakup time of a filament of component 1 surrounded by a matrix of component 2 should equal the break-up time of a filament of component 2 surrounded by a matrix of component 1. The result is[25]:

$$\frac{\phi_1}{\phi_2} = \frac{\eta_1}{\eta_2} F\left(\frac{\eta_1}{\eta_2}\right) \tag{3}$$

in which $F(\eta_1/\eta_2) = 1 + 2.25\log(\eta_1/\eta_2) + 1.81[\log(\eta_1/\eta_2)]^2$.

Utracki[24] used a theory which describes the influence of dispersed particles on the viscosity of a liquid. Phase inversion is assumed to occur if the viscosity of dispersion of component 1 in component 2 equals the viscosity of dispersion of component 2 in component 1. The result is:

$$\phi_2 = \frac{1}{2}\left(1 - \frac{\log(\frac{\eta_1}{\eta_2})}{[\eta]}\right) \tag{4}$$

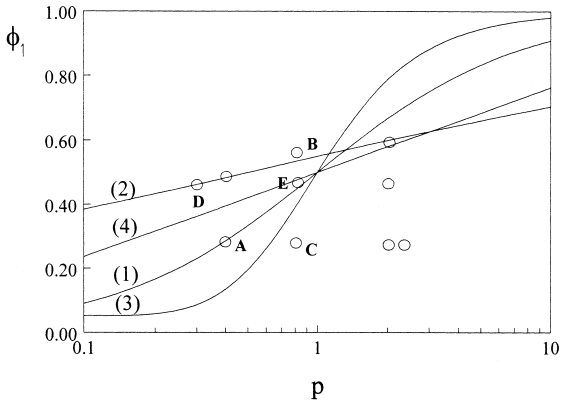

Figure 1 Volume fraction at phase inversion of a binary blend as a function of the viscosity ratio, p, according to equations (1)–(4). ○, experimental results (A–E are described in this paper; other points are described in Ref.[34]

in which $[\eta]$ is a dimensionless intrinsic viscosity of the dispersed phase. A value of $[\eta] = 1.9$ was chosen in order to fit experimental results. The results of both theories are also shown in *Figure 1*.

Equations (1) to (4) describe the phase inversion as a function of the viscosity ratio, $p = \eta_1/\eta_2$. Given the experimental results found in the literature[24] and our own results (the latter are shown in *Figure 1*), it appears that the viscosity ratio alone is not sufficient to predict the phase inversion point in all circumstances (different materials and different processing conditions). Apparently, other parameters, e.g. the interfacial tension, absolute values of the viscosities rather than their ratio, phase dimensions and mixing conditions have an effect on the formation of co-continuous structures. These parameters are not taken into account in equations (1) to (4). Moreover, equations (1) to (4) just give a single composition for phase inversion, whereas experimentally a range of compositions is found for fully co-continuous structures. For these reasons, a new model is developed, introducing the dependence of the formation of the co-continuous morphology on material properties and processing conditions via the consideration of the shape of the dispersed phase required for achieving co-continuity.

A simplified picture of full co-continuity

The relations described above do not take into consideration any requirements as to the shape of the dispersed phase. However, in order for the minor phase to become continuous inside the major phase, certain requirements for its shape should be satisfied. Suppose that 10 vol% of component 1 in 90 vol% of component 2 gives a co-continuous morphology. This can never be achieved if the minor phase is present in the form of spherical droplets, because the randomly distributed droplets will not touch one another. Above 16 vol% droplets, percolation will occur[18], but a fully continuous phase will be formed only when the maximum packing density of spheres is reached ($\approx$ 70 vol% spheres, depending on the type of packing). In order to obtain a continuous phase at low volume fractions of component 1 (0–50 vol%), its particles must be elongated. For finding the volume fraction, where a fully co-continuous morphology can exist, a practical approach is to consider the minor phase at this volume fraction as randomly oriented rodlike particles at their maximum packing density. At this density, all the rods will touch, which is a prerequisite for full co-continuity. Representing co-continuous structures by a packing of rodlike particles is, admittedly, a gross simplification. In true co-continuous structures, the rods have 'coalesced' at their cross-over points and may have extremely non-circular cross-sections. However, this simple model captures the essential geometrical conditions for continuity of a minor phase. So, in our approach, the dispersed minor phase will become fully continuous, as soon as the maximum packing density for its shape is reached.

The maximum packing density (ϕ_{max}) of randomly oriented rods depends on the aspect ratio L/B, where L is the length and B is the diameter of the particle. The following empirical relation can be found in the literature[27] for the maximum packing density of randomly oriented stiff rods:

$$\frac{1}{\phi_{max}} = 1.38 + 0.0376\left(\frac{L}{B}\right)^{1.4} \tag{5}$$

For spheres (aspect ratio of 1), ϕ_{max} is 0.7. The maximum packing density will decrease when the aspect ratio increases, e.g. randomly oriented rods with an aspect ratio of 16 have a maximum packing density of only 0.31. The maximum packing density given by equation (5) is the minimum volume fraction of the minor component at which full co-continuity can exist for the given L/B. The upper bound for the composition range of full co-continuity is also given by equation (5), if it is applied to the other component. This consideration leads to a composition range for the existence of full co-continuity, as is found experimentally. This is in contrast to equations (1) to (4), which only define a phase inversion point.

With this model, the volume fraction for the phase inversion point, or, more accurately, the lower limit for co-continuous morphologies, becomes a function of the parameter L/B. It is not a function of the viscosity ratio, p. It is illustrative, however, to present this volume fraction, ϕ_{max}, in a 3D-plot as a function of L/B and p in order to enable a comparison with equations (1) to (4). *Figure 2* shows ϕ_1 as a function of the aspect ratio L/B, derived from equation (5) with $\phi_1 = \phi_{max}$, and the viscosity ratio ($0.1 < p < 1$). Although there is no dependency on p, the figure serves to illustrate that equation (1) equation (2) equation (3) equation (4) require different values of L/B at the phase inversion point. This can be shown by projecting the curves of *Figure 1* onto the surface in *Figure 2*. For example, at $p = 0.5$, equation (1) requires an aspect ratio for the elongated particles of at least 15, whereas equation (2) only requires a ratio of about 7.

In the present approach, the parameter L/B follows from purely geometrical considerations. It results from the requirement that particles of the minor phase should have an elongated shape in order to be continuous at low volume fractions. This shape should also be stable during processing. This stability is determined by the interfacial tension of the system, phase dimensions, values of the viscosities and mixing conditions. In this way, the parameter L/B introduces the effects of all these parameters on the limits of the composition region between which co-continuity can be found. Since each equations (1) to (4) and all other possible ones must obey the purely geometrical conditions for co-continuity, the effect of the above mentioned parameters on L/B will also lead to finding the conditions for validity of these relations.

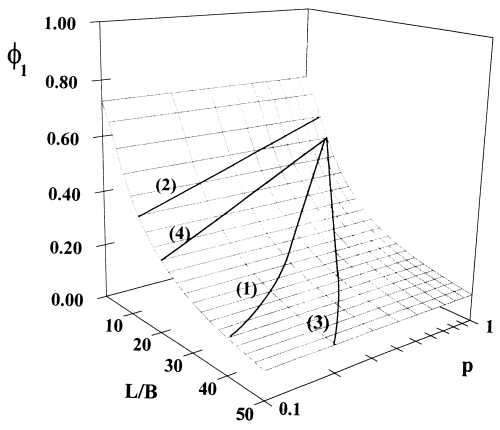

Figure 2 Volume fraction at phase inversion as a function of the viscosity ratio, p, and the aspect ratio, L/B, according to equation (9). The lines represent the projections of equations (1)–(4) to illustrate that they require different values of L/B

Conditions for the stability of elongated particles

During the mixing process, the domains of each component are deformed by the applied flow field. The deformation results in elongated particles of the dispersed phase. It was shown above that elongated particles are needed for the formation of a fully continuous phase below a volume fraction of 0.7. In this section, it is attempted to establish the conditions for the stability of these elongated particles.

Co-continuity is obtained when the aspect ratio of the deformed particles becomes such that their volume fraction, ϕ_d, is equal to $\phi_{max}(L/B)$ given by equation (5). Whether such aspect ratios can exist depends on the local capillary number, which is given by:

$$Ca = \frac{\eta_m \dot{\gamma} B}{2\sigma} \tag{6}$$

where σ is the interfacial tension, η_m is the viscosity of the matrix phase and $\dot{\gamma}$ is the shear rate.

We start by examining a domain of the minor component of the equivalent sphere diameter $2R_0$ as it deforms into a long cylinder and changes its L/B in a given flow field. The diameter, B, of the cylinder is a function of the deformation, and, therefore, the aspect ratio (conservation of volume):

$$\frac{B}{2R_0} = \left(\frac{2}{3}\right)^{1/3} \left(\frac{L}{B}\right)^{-1/3} \tag{7}$$

By using equation (7), the capillary number becomes:

$$Ca = \frac{\left(\frac{2}{3}\right)^{1/3} \eta_m \dot{\gamma} R_0 \left(\frac{L}{B}\right)^{-1/3}}{\sigma} \tag{8}$$

During the flow in the mixer at high values of Ca, the shear stress overrules the interfacial stress and the particles are stretched. As L/B increases, Ca decreases. When a critical value, Ca_{crit}, is reached, the interfacial stress destabilizes the elongated particles and break-up occurs. The mixing process can thus be divided into two regimes[28]:

(1) Distributive mixing: $Ca > > Ca_{crit}$. The drops are extended (affinely) into long slender threads. A disturbance at the surface of the thread does not lead to break-up because the shear stress is much larger than the local interfacial stress. The elongating particles are stable, consequently a co-continuous morphology can be generated over a wide range of compositions.
(2) Dispersive mixing: $Ca \approx Ca_{crit}$. The interfacial stress is important here. Disturbances at the surface of the thread will grow, leading to break-up into smaller droplets. The elongating particles are not stable during flow. Co-continuous morphologies can exist only at high volume fractions.

Grace[29] found that Ca_{crit} is a function of the viscosity ratio, $p = \eta_d/\eta_m$, where η_d and η_m are the viscosities of the dispersed and matrix phase, respectively. His results are valid for Newtonian droplets under equilibrium conditions and for a mechanism of a droplet breaking into two smaller droplets, so it is doubtful whether they are applicable to polymer mixing processes. A more realistic break-up mechanism appears to be one where a relatively large droplet ($Ca > Ca_{crit}$) is stretched into a thread that may break up into a line of smaller droplets[30]. The threads are stable during stretching until the interfacial stress overrules the shear stress ($Ca = 1$) and break-up occurs. For that reason, the value $Ca_{crit} = 1$ is used here as the boundary

between the distributive and dispersive mixing regions, and as the limit for the existence of the extended structures that can form continuous phases.

The discussion of the conditions for the formation of elongated structures has been limited so far to a single isolated particle. Neither multi-particle interactions nor the influence of coalescence have been accounted for, which must occur if a co-continuous structure is imagined to be formed from elongated droplets. By using the capillary number in the fashion described above, however, it is not implied that the mechanism of formation of the co-continuous morphology should be a deformation of droplets to threads, which subsequently are closely packed and which locally coalesce. In reality, the formation of co-continuous structures more likely proceeds by a sheet-forming mechanism[31,32], involving break-up and local coalescence of sheets of the minor component. The condition $Ca > 1$ given above regards the possible stability of elongated structures, whatever their origin.

New relation for co-continuity

As stated above, a co-continuous morphology may be modelled by a dense packing of elongated particles. The lower limit of the volume fraction where a full co-continuous phase can be found is given as a function of the aspect ratio by equation (5). The condition for existence of such elongated particles is $Ca > 1$, where Ca is given by equation (8). Although strictly speaking these two equations are relevant in different situations (dense packing versus isolated drops), by combining these equations for $Ca = 1$ we obtain an approximate expression, giving the lower limit for co-continuity in terms of σ, η_m, $\dot{\gamma}$ and R_0:

$$\frac{1}{\phi_{d,cc}} = 1.38 + 0.0213\left(\frac{\eta_m \dot{\gamma}}{\sigma} R_0\right)^{4.2} \qquad (9)$$

In *Figure 3*, the limit for co-continuity according to equation (9) is shown, demonstrating the strong dependence of $\phi_{d,cc}$ on $\eta_m \dot{\gamma}/\sigma$ and R_0, a size which is determined by the particulars of the blending process. From this figure, it appears that co-continuity is possible even at low volume fractions provided $\eta_m \dot{\gamma}/\sigma$ or R_0 are high enough. As the typical phase dimensions in polymer blending are approximately 1 μm ($2R_0 = 1$ μm), co-continuity will be possible at volume fractions below 0.5 provided $\eta_m \dot{\gamma}/\sigma$ exceeds 4.4×10^6 m^{-1} in order to get elongated particles ($L/B > 8$ in this case). This can be achieved by a proper choice of the polymers used (η_m) and the blending conditions ($\dot{\gamma}$). For example, for a blend with $\sigma = 5$ mN/m, $2R_0 = 1$ μm and $\dot{\gamma} = 20$ s^{-1}, the viscosity of the matrix phase should exceed 1000 Pa.s.

Equation (9) does not include p as an independent variable, whereas the equations (1) to (4), used so far, show a dependency on p only. An apparent dependence of $\phi_{d,cc}$ on p closely resembling equation (3) can be obtained only if the viscosity of the dispersed phase is kept constant and the viscosity of the matrix is varied. This is illustrated in *Figure 4* using values for η_m, $\dot{\gamma}$, σ and R_0 as experimentally found for the system PS/PE described in the next section. If the viscosity of the matrix is kept constant and the viscosity of the dispersed phase is varied, $\phi_{d,cc}$ is independent of p. This is also illustrated in *Figure 4*. In fact, all sorts of apparent dependencies of $\phi_{d,cc}$ on p can be obtained experimentally depending on the way η_m and η_d are varied in the experiments. This explains why some experimental results do not support any of equations (1) to (4), while others do.

Equation (9) gives the lower limit of the range of volume fractions within which a co-continuous structure can exist. The upper limit will be given by an analogous formula in which the two components of the blends have changed role. As stated previously in relation to equation (5), this consideration naturally leads to a composition range for existence of full co-continuity, as is found experimentally.

EXPERIMENTAL

Two grades of polystyrene (PS) and two grades of low density polyethylene (PE), shown in *Table 1*, were used to prepare the blend series shown in *Table 2*. Nine different compositions (10–90 wt% PS in PE) were made by extrusion at 200 and 250°C. The mixing equipment consisted of a 20 mm Collin laboratory extruder equipped with a transport screw, and a static mixer in series with the extruder containing 10 Ross ISG 15 mm diameter mixing elements. Each element contains four channels with a radius of 0.135 cm. The average shear rate in the channels was estimated to be 22 s^{-1}. The extruded strands were quenched in water.

A Rheometrics RMS-800, operating in the plate/plate

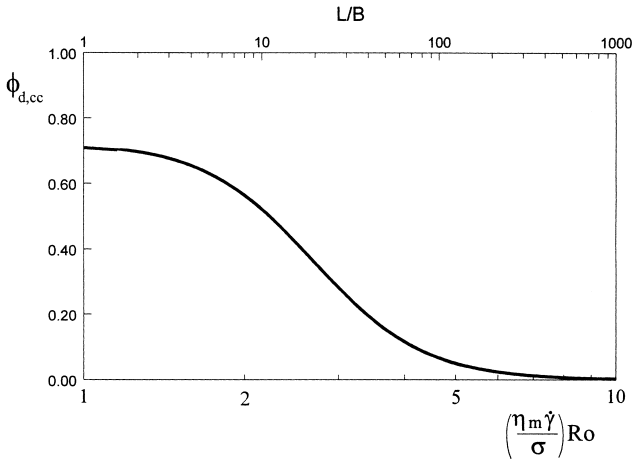

Figure 3 Composition at onset of co-continuity as a function of $(\eta_m \dot{\gamma}/\sigma)\cdot R_0$ according to equation (9) and of L/B according to equation (5)

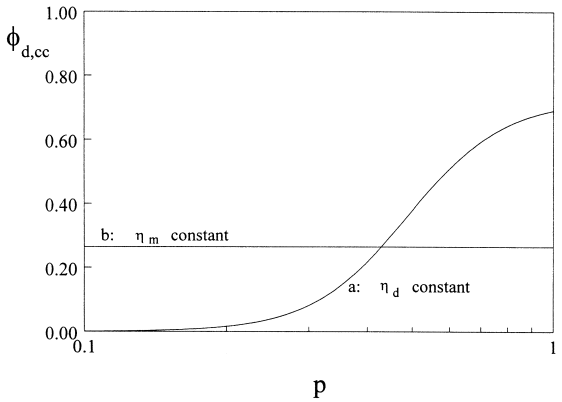

Figure 4 Apparent dependence of the compositions at which co-continuity is possible on p according to equation (9); the viscosities are varied: (a) η_d = 900 Pa.s, η_m = 900–9000 Pa.s and (b) η_m = 1800 Pa.s, η_d = 180–1800 Pa.s; in both cases: σ = 4.5 mN/m; $\dot{\gamma}$ = 22 s^{-1}; $2R_0$ = 0.7 μm

Table 1 Trade names and shear viscosities at $\dot{\gamma} = 22\ s^{-1}$ of the polymers used

Sample code	Trade name (manufacturer)	Viscosity (Pa.s) at 200°C	Viscosity (Pa.s) at 250°C
PS1	Hostyrene N2000 (Shell)	780	160
PS2	Styron 678E (DOW)	1440	380
PE1	Stamylan LD 2100TN00 (DSM)	1860	1210
PE2	Stamylan LD 2102TN26 (DSM)	960	540

Table 2 Blends studied in this work, the viscosity ratio of the components, their expected inversion points (vol%) according to equation (1) and equation (2), and the volume fractions for the lower limit of co-continuity according to equation (9) and measured experimentally

Series	Blend components	T(°C)	p	ϕ_1 (vol %) [equation (1)]	ϕ_1 (vol %) [equation (2)]	$\phi_{d,cc}$ (vol %) [equation (9)]	$\phi_{v,PS}$ (vol%) (experimental)
A	PS1,PE1	200	0.4	30	48	25	27
B	PS1,PE2	200	0.8	45	53	64	56
C	PS2,PE1	200	0.8	44	53	25	27
D	PS1,PE2	250	0.3	24	46	46	46
E	PS2,PE2	250	0.7	41	52	46	46

configuration, was used to measure the rheological behaviour of the polymers. The measurements were carried out in the angular frequency range of 0.1–100 rad/s with a strain of 5%. The Cox–Merz rule appeared to be valid. The viscosities of the polymers at 22 s^{-1} for temperatures of 200 and 250°C are given in *Table 1*.

The interfacial tension between PE and PS at 200°C is 4.5 mN/m, determined both experimentally[30] and theoretically[33]. The calculated value at 250°C is 3.5 mN/m[33].

Co-continuity in the blends was checked by extraction experiments. The strands were broken in liquid nitrogen and extraction of the PS phase was performed in a Soxhlet extraction apparatus with 2-butanon for three days. This was sufficient for complete removal of the soluble fraction. The samples were checked as to whether they were self-supporting after extraction. Five pieces of the extruded strands were used to obtain an average value. In the case of co-continuity, 100% of the PS phase can be extracted. It was not possible to extract the LDPE phase without damaging the PS phase. For that reason, the upper limit for the composition range of co-continuity could not be determined. In all reported experiments, PE is the matrix phase. A scanning electron microscope (Philips XL 20) was used to study the phase dimensions after extraction. The droplet radii and filament thicknesses given are the results of 50–100 measurements of the holes resulting from the extraction.

RESULTS AND DISCUSSION

The main experimental results obtained for the different blends are summarized in *Table 2* together with the calculated compositions for the onset of full co-continuity according to equation (9), and the calculated phase inversion points according to equation (1) and equation (2). The experimental results shown in this paper demonstrate the influence of variations in viscosities on the composition for co-continuity, as will be discussed in detail below. Experimental results regarding the influences of the interfacial tension will be reported separately[34].

Constant viscosity of the dispersed phase

Increasing the matrix viscosity leads to more stable filaments of the minor phase, and co-continuity is possible at lower volume fractions. It was shown in *Figure 4* that only then the composition, where co-continuity is possible, appears to depend on the viscosity ratio. This calculated trend was checked by comparing the blends of series A and B, made at 200°C. The matrix viscosity in series A is twice as high as in series B. If the phase dimensions are the same, then co-continuity in the blends of series A is expected at a lower volume fraction than in the blends of series B made under the same conditions, according to equation (9) and

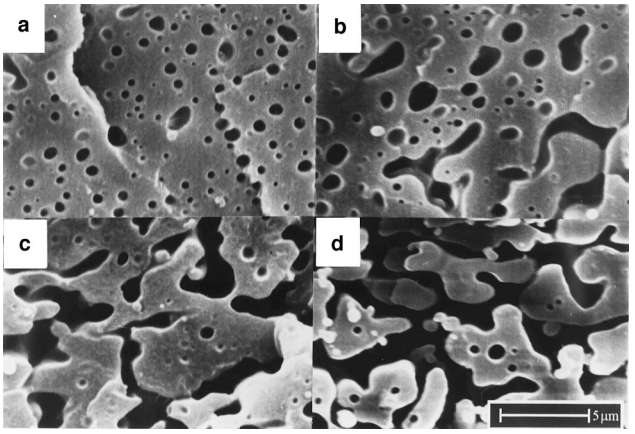

Figure 5 Scanning Electron Micrographs of blends of series A; (a)–(d) contain 17, 27, 35 and 46 vol% PS, respectively

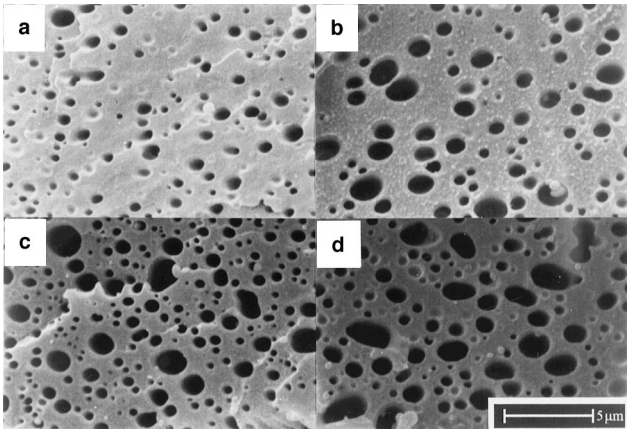

Figure 6 Scanning Electron Micrographs of blends of series B; (a)–(d) as in *Figure 5*

Figure 3. SEM pictures of several compositions are shown in *Figures 5 and 6*. As shown in *Table 3*, no significant difference of the phase dimensions is found between the blends of series A and B, despite the differences in viscosity ratio. Elongated structures are found from 27 vol% PS and higher in the blends of series A, whereas in the blends of series B a dispersion of droplets is found up to 46 vol% PS.

The results of the extraction experiments are given in *Table 4*. The blends containing 80 and 90 wt% PS were not self-supporting after extraction, and were not taken into consideration. Co-continuity was found at 27 vol% PS for series A ($p = 0.4$) and at 56 vol% PS for series B ($p = 0.8$).

The new model uses the value of the capillary number in the mixer to predict the type of morphology. The values of *Ca* based on the average size of the PS domains in the blend are given in *Table 5*. It is clear from this table that the blends of series A have experienced distributive mixing at every composition ($Ca > 1$). Co-continuous morphologies can be expected at all these compositions. In reality, co-continuity starts at 27 vol% PS. The capillary number in series B based on the average phase diameter is also larger than 1 in all blends. Extraction results show that co-continuity does not start until 56 vol% PS.

The results presented above demonstrate that the average diameter of the filaments is not the best measure of the phase dimensions to be used in the capillary number. In a real blend there is a distribution of sizes (*Figures 5 and 6*). The thinnest filaments can experience dispersive mixing because their capillary number is much lower than the average value. They will break and destroy the phase continuity. The stability of the morphology is determined by the existence of these thin filaments and not by the average size. So, it is the minimum diameter measured in the sample that should be used in the capillary number to assess the conditions for full co-continuity.

Equation (6) can also be used to calculate the minimum stable diameter by introducing the condition $Ca = 1$ and solving for B. For the blends of series A, a value of $B = 0.22\ \mu$m is found. All filaments thinner than 0.22 μm will break up in the mixer and destroy the co-continuous morphology. One can see from *Table 3* that such thin filaments hardly exist in the blends of series A at 27 vol% PS or more. Consequently, these blends are co-continuous. The minimum stable filament diameter for the blends of series B, on the other hand, is 0.44 μm. In *Table 3*, we can see that thinner filaments are present in these blends up to 46 vol% PS. Above this value, these thin filaments are no longer present and co-continuity is possible. Co-continuity was found to start at 56 vol% PS.

Although even the minimum capillary number is larger than 1, no co-continuity was found at volume fractions lower than 27 vol% for series A. SEM pictures show that no elongated structures are found at these compositions (*Figure 5*). The measured phase dimensions at these compositions, however, are not only filament thicknesses, but also the diameters of the droplets formed by break-up of the thinnest filaments. When a filament is broken, the resulting droplets have twice the diameter of the original filament. This leads to an apparently higher minimum capillary number in the blends.

Constant viscosity of the matrix phase

The calculations for *Figure 4* showed that a constant matrix viscosity should give a constant composition at which co-continuity is possible, independent of the viscosity of the dispersed phase. In order to check this calculated trend, the results of the blends of series A and C are compared. Co-continuity in series A was found at 27 vol%

Table 3 Number average local diameter, B, and the standard deviation (in μm), of the PS phase measured in the blends

Vol% PS	A	B	C	D	E
9	0.43 ± 0.17	0.52 ± 0.19	0.47 ± 0.24	0.57 ± 0.27	0.44 ± 0.16
17	0.49 ± 0.16	0.56 ± 0.22	0.51 ± 0.22	0.57 ± 0.25	0.43 ± 0.18
27	0.61 ± 0.33	0.64 ± 0.27	0.64 ± 0.30	0.68 ± 0.31	0.65 ± 0.22
35	0.84 ± 0.35	0.76 ± 0.35	0.61 ± 0.25	0.90 ± 0.54	0.71 ± 0.29
46	0.99 ± 0.39	0.84 ± 0.39	0.98 ± 0.40	1.50 ± 0.60	1.43 ± 0.6

Table 4 Percentage of PS extracted from the blends as a function of the volume fraction

Vol%PS	A	B	C	D	E
9	22 ± 7	24 ± 1	25 ± 5	18 ± 1	16 ± 1
17	86 ± 3	34 ± 4	72 ± 9	31 ± 4	18 ± 1
27	99 ± 2	77 ± 2	100	60 ± 12	60 ± 10
35	100	94 ± 4	100	92 ± 2	86 ± 4
46	100	93 ± 2	100	99 ± 2	100
56	100	100	100	100	100
66	100	100	100	100	100

Table 5 Capillary number calculated from the local diameter of the PS phase in the blends as a function of the volume fraction

Vol % PS	A	B	C	D	E
9	2.0 ± 0.8	1.2 ± 0.4	2.1 ± 1.0	1.0 ± 0.5	0.7 ± 0.2
17	2.2 ± 0.8	1.3 ± 0.5	2.3 ± 1.0	1.0 ± 0.5	0.7 ± 0.3
27	2.8 ± 1.5	1.5 ± 0.7	2.9 ± 1.3	1.2 ± 0.6	1.1 ± 0.4
35	3.8 ± 1.6	1.8 ± 0.9	2.8 ± 1.2	1.5 ± 0.9	1.2 ± 0.5
46	4.5 ± 1.7	2.0 ± 0.9	4.5 ± 1.9	2.5 ± 1.0	2.4 ± 1.0

PS (*Table 4*). *Table 3* indicates that no significant difference of the phase dimensions is found between series A and C, and the blends of series C have also experienced distributive mixing (*Table 5*). Co-continuity in series C should, therefore, also be expected at 27 vol% PS, something that is verified by the extraction results, given in *Table 4*. At this volume fraction, elongated structures are found as shown in *Figure 7*. These elongated structures and co-continuity, on the other hand, are not found in blends of series B, which have about the same viscosity ratio, but a lower matrix viscosity.

The comparison of series A and C demonstrates that varying the viscosity of the dispersed phase does not affect the composition at which co-continuity is found, in agreement with *Figure 4*.

Lower matrix viscosities will shift co-continuity to higher volume fractions of the dispersed phase according to *Figure3*. This was investigated experimentally by making blends at 250°C with PE2 as the matrix. At this temperature, the viscosity ratios of the components of series D and E are similar to the ones of the blends A and C, respectively, while the interfacial tension hardly changed. *Figure 8* shows the morphologies for series D at this temperature. No elongated structures were found, until the PS phase becomes continuous at 46 vol% PS. Images similar to those in *Figure 8* were obtained for series E. The phase dimensions are given in *Table 3*.

No significant difference in the phase dimensions is found by increasing the temperature from 200 to 250°C, except for the 46 vol% PS blends (*Table 3*). The calculated capillary numbers are given in *Table 5*. At both viscosity ratios, the blends D and E with less then 46 vol% PS have experienced dispersive mixing. The 46 vol% PS blends have experienced distributive mixing, and co-continuous morphologies were indeed found at this composition for both blends (*Table 4*). The diameter of the thinnest stable filament in these blends, calculated with equation (6), is $B = 0.59\ \mu$m. Only at 46 vol% PS were thinner filaments absent. These results show that lower viscosities (250°C) at a constant viscosity ratio shift the co-continuity range to higher volume fractions. For example, at $p = 0.3$–0.4, the composition at which co-continuity is found shifts from 27 vol% PS (series A made at 200°C) to 46 vol% PS (series D made at 250°C), when the matrix viscosity is reduced by a factor of 3.5.

The volume fractions at which co-continuity was found experimentally are shown in *Figure 9* as a function of $\eta_m\,\dot{\gamma}/\sigma$ and $2R_0$. Co-continuity in the blends of series A, B and C can be described by equation (9) if $2R_0 = 0.7\ \mu$m. Co-continuity in the blends of series D and E can be described by equation (9) if $2R_0 = 1.4\ \mu$m. From the SEM pictures it can be seen that the minimum phase diameters in the blends of series D and E in the case of co-continuity were indeed twice as large as those in series A, B and C.

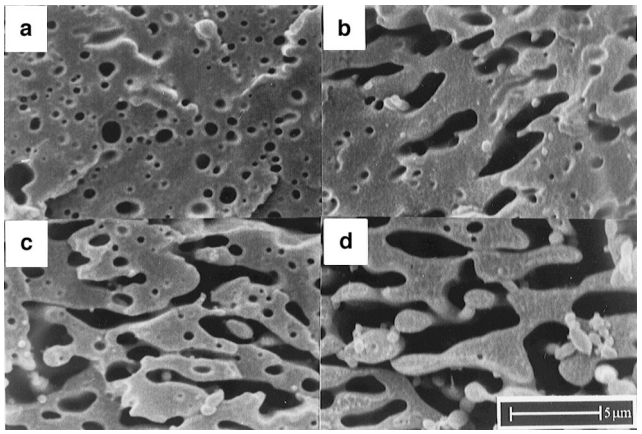

Figure 7 Scanning Electron Micrographs of blends of series C; (a)–(d) as in *Figure 5*

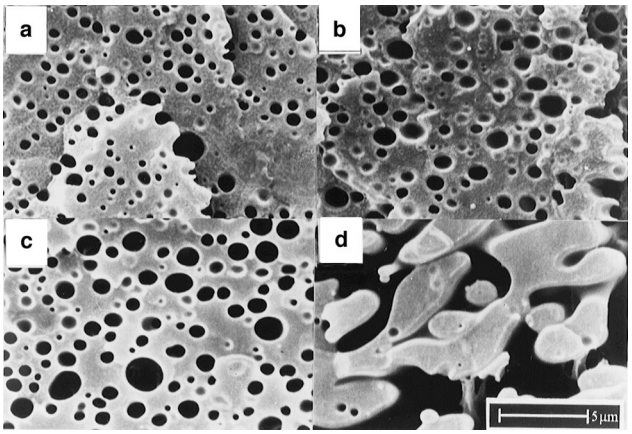

Figure 8 Scanning Electron Micrographs of blends of series D; (a)–(d) as in *Figure 5*

GENERAL DISCUSSION

In the past, co-continuity has usually been associated with phase inversion. A number of relations have been proposed relating the composition for phase inversion to the viscosity ratio of the polymers. These relations obviously are insufficient to describe experimental results, as illustrated in *Figure 1*. Fully co-continuous structures may indeed be expected to occur at the composition where the matrix and dispersed phase change role. However, this may well be the case over a range of compositions (e.g. Ref.[18]). As co-continuity requires a certain well-defined degree of distribution of the components of the blend, it is to be expected that the classical parameters governing formation

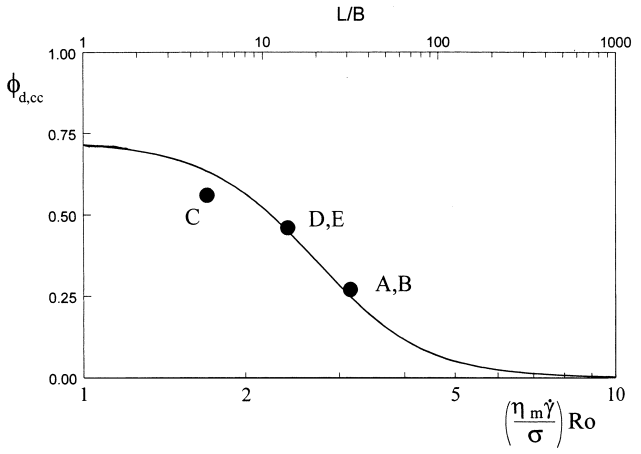

Figure 9 Comparison of the experimental results of series A–C ($2R_0 = 0.7\ \mu$m), and of series D and E ($2R_0 = 1.4\ \mu$m), with the curve that describes the composition at which co-continuity is possible as a function of $(\eta_m\,\dot{\gamma}/\sigma)\cdot R_0$ [equation (9)]

of dispersion, e.g. shear rate, viscosity and interfacial tension, should determine the composition range for co-continuity.

Full co-continuity at low volume fractions of the dispersed component can exist only provided this component is dispersed in a network-like structure with ligaments of sufficiently large aspect ratio. The relation between composition and aspect ratio employed in this paper stems from experimental results on systems which are only analogous to our systems, but certainly different in geometrical detail. Clearly one can envisage a more sophisticated approach than the empirical result expressed by equation (5), e.g. a mathematical model based on a network theory using network strands of certain aspect ratios. However, the essential point that there is a dependency of the concentration for onset of full co-continuity on the aspect ratio of the ligaments is well expressed in equation (5).

In order to determine the possible stability of the extended structural elements, we have used the classical approach of the local capillary number. This, again, is an approximation, since the condition expressed in the limiting capillary number holds only for isolated dispersed particles, whereas the ligaments to which this condition is applied form a dense network. In the derivation of equation (9) we have not made any assumption regarding the mechanism of blending or the mechanism of formation of co-continuous structures. We have merely combined the geometrical conditions for the existence of co-continuous structures with micro-rheological conditions for stability of the weakest parts of these structures, the ligaments.

This results in a relation [equation (9)] which has two essential properties, i.e. (i) it relates the composition of the existence of co-continuous structures to blending conditions and micro-rheological properties; and (ii) it naturally leads to a range of compositions. Equation (9) has neither the viscosity ratio nor the viscosity of the dispersed phase as an explicit variable. From the independence of $\phi_{d,cc}$ of η_d, one should, however, not conclude that the blending process itself is independent of η_d. Both viscosities, of course, play a role in the blending process, and η_d seems to be a factor in determining the magnitude of R_0 via the process of sheet break-up, although for a given combination of polymers (e.g. PE/PS), R_0 does not appear to vary a great deal[35]. The experimental results presented in this paper confirm that $\phi_{d,cc}$ is largely independent of η_d.

The parameters η_m, $\dot{\gamma}$ and σ on one hand, and R_0 on the other, differ in as much that the former can be determined *a priori*, whereas the latter has to be measured afterwards. Consequently, our model cannot be used in a predictive manner. A prediction of the phase dimensions, and in particular the minimum phase dimensions, requires detailed knowledge of the blending process. Several attempts have been made to predict the final particle size in blending processes (e.g. Refs[36–38]), generally with limited success. For a reliable prediction of the phase dimensions, a description of the morphology development in the mixing equipment is required. Currently, opinion prevails that in the early stages of polymer blending, a quick morphology change occurs by a mechanism of sheet formation[31,32]. Some results for single screw extrusion showing sheet break-up to be the decisive factor in determining the final phase dimensions will be published shortly[35]. A quantitative modelling of this 'sheeting' mechanism would enable a prediction of R_0 and, consequently, of the critical volume fraction for full co-continuity.

CONCLUSION

Geometrical requirements have to be fulfilled for co-continuous structures to exist at low volume fractions of the minor component. An empirical expression originally derived for glass-fibre-filled systems can be used for describing the volume fraction for the onset of full co-continuity as a function of the aspect ratio. Combination of the geometrical requirements with micro-rheological conditions for stability of extended structures leads to a new relation describing the critical volume fraction of the minor phase as a function of the matrix viscosity, interfacial tension, shear rate and phase dimensions. This relation implies a range of compositions within which fully co-continuous structures can exist. Experimental evidence for the system PE/PS shows that the model quantitatively predicts trends in the critical volume fraction as a function of the viscosities of the polymers. The critical volume fraction does not depend on the viscosity of the dispersed phase. The phase dimensions have to be measured afterwards, the minimum strand thickness is shown to be the relevant size.

ACKNOWLEDGEMENTS

Thanks are expressed to the Dutch Ministry of Economic Affairs (IOP/Recycling) for the financial support of this research.

REFERENCES

1. Seo, Y., Hwang, S. S. and Kim, K. U., *Polymer*, 1993, **34**, 1667.
2. Borggreve, R. J. M., Ph.D. thesis, Twente University of Technology, The Netherlands, 1986.
3. Wu, S., *Polymer*, 1985, **26**, 1855.
4. Crevecoeur, G., Ph.D. thesis, Katholieke Universiteit, Leuven, Belgium, 1991.
5. Shin, B. Y., Jang, S. H., Chung, I. J. and Kim, B. S., *Polym. Engng Sci.*, 1992, **32**, 73.
6. Roetting, O. and Hinrichsen, G., *Adv. Polym. Technol.*, 1994, **13**, 57.
7. Machiels, A. G. C., Denys, K. F. J., Van Dam, J. and Posthuma de Boer, A., *Polym. Engng Sci.*, 1996, **36**, 2451.
8. Machiels, A. G. C., Denys, K. F. J., Van Dam, J. and Posthuma de Boer, A., *Polym. Engng Sci.*, 1997, **37**, 59.
9. Verhoogt, H., Willems, C. R. J., Van Dam, J. and Posthuma de Boer, A., *Polym. Engng Sci.*, 1994, **34**, 453.
10. Nir, M. B., Ram, A. and Miltz, J., *Polym. Engng Sci.*, 1995, **35**, 1878.
11. Gergen, W. P., Lutz, R. and Davison, S., in *Thermoplastic Elastomers: A Comprehensive Review*, eds N. R. Legge, G. Holden and S. Davison. Carl Hanser, Munich, Germany, 1987, pp. 507–540.
12. Gergen, W. P. and Davison, S., U.S. Patent 4,041,103, 1977.
13. Xie, H. Q., Xu, J. and Zhou, S., *Polymer*, 1991, **32**, 95.
14. Verhoogt, H., Ph.D. thesis, Delft University of Technology, The Netherlands, 1992.
15. Nelson, C. J., Avgeropoulos, G. N., Weissert, F. C. and Böhm, G. G. A., *Angew. Makromol. Chem.*, 1977, **60/61**, 49.
16. Valenza, A., Demma, G. B. and Acierno, D., *Polym. Networks Blends*, 1993, **3**, 15.
17. Favis, B. D. and Chalifoux, J. P., *Polymer*, 1988, **29**, 1761.
18. Lyngaae-Jørgensen, J. and Utracki, L.A., *Makromol. Chem., Macromol. Symp.*, 1991, **48/49**, 189.
19. Paul, D. R. and Barlow, J. W., *J. Macromol. Sci., Rev. Macromol. Chem.*, 1980, **C18**, 109.
20. Jordhamo, G. M., Manson, J. A. and Sperling, L. H., *Polym. Engng Sci.*, 1986, **26**, 517.
21. Miles, I. S. and Zurek, A., *Polym. Engng Sci.*, 1988, **28**, 796.
22. Avgeropoulos, G. N., Weissert, F. C., Biddison, P. H. and Böhm, G. G. A., *Rubber Chem. Technol.*, 1976, **49**, 93.
23. Ho, R. M., Wu, C. H. and Su, A. C., *Polym. Engng Sci.*, 1990, **30**, 511.

24. Utracki, L. A., *Polym. Mater. Sci. Engng*, 1991, **65**, 50.
25. Metelkin, V. I. and Blekht, V. S., *Colloid J. USSR*, 1984, **46**, 425.
26. Tomotika, S., *Proc. Roy. Soc. (London)*, 1935, **A150**, 322.
27. Cross, M. M., Kaye, A., Stanford, J. L. and Stepto, R. F. T., *Polym. Mater. Sci. Engng; Proceedings of the ACS*, 1983, **49**, 531.
28. Janssen, J. M. H., Ph.D. thesis, Eindhoven University of Technology, The Netherlands, 1993.
29. Grace, H. P., *Chem. Engng Commun.*, 1982, **14**, 225.
30. Elmendorp, J. J., Ph.D. thesis, Delft University of Technology, The Netherlands, 1986.
31. Scott, C. E. and Macosko, C. W., *Polymer*, 1992, **36**, 461.
32. Sundararaj, U., Macosko, C. W., Rolando, R. J. and Chan, H. T., *Polym. Engng Sci.*, 1992, **32**, 1814.
33. Wu, S., *Polymer Interface and Adhesion*, Marcel Dekker, New York, 1982.
34. Willemse, R. C., Posthuma de Boer, A., Van Dam, J., Gotsis, A. D., *Polymer*, accepted.
35. Willemse, R. C., Ramaker E. J. J., Van Dam, J. and Posthuma de Boer, A., *Polymer* (submitted).
36. Taylor, G. I., *Proc. Roy. Soc. (London)*, 1932, **A138**, 41.
37. Wu, S., *Polym. Engng Sci.*, 1987, **27**, 335.
38. Baird, D. G. and Collias, D. I., *Polymer Processing*, Butterworth-Heinemann, Boston, 1995, pp. 135–177.